Bioconjugate Chemistry

Article

Covalent Conjugation of Small-Molecule Adjuvants to Nanoparticles Induces Robust Cytotoxic T Cell Responses via DC Activation

Woo Gyum Kim, Bongseo Choi, Hyun-Ji Yang, Jae-A Han, Hoesu Jung, HyungJoon Cho, Sebyung Kang, and Sung You Hong

Bioconjugate Chem., **Just Accepted Manuscript** • DOI: 10.1021/acs.bioconjchem.6b00277 • Publication Date (Web): 09 Aug 2016

Just Accepted

ACS Publications

Bioconjugate Chemistry is published by the American Chemical Society. 1155 Sixteenth Street N.W., Washington, DC 20036

Covalent Conjugation of Small-Molecule Adjuvants to Nanoparticles Induces Robust Cytotoxic T Cell Responses via DC Activation

Woo Gyum Kim,[†,§] Bongseo Choi,[‡,§] Hyun-Ji Yang,[†] Jae-A Han,[‡] Hoesu Jung,[‡]

HyungJoon Cho,[‡] Sebyung Kang,[‡,*] and Sung You Hong[†,*]

[†]School of Energy and Chemical Engineering and [‡]School of Life Sciences, Ulsan National Institute of Science and Technology (UNIST), UNIST-gil 50, Ulsan 689-798, Republic of Korea

ABSTRACT: Specific recognitions of pathogen associated molecular patterns by Toll-like receptors (TLRs) initiate dendritic cell (DC) activation, which are critical for coordinating innate and adaptive immune responses. Imidazoquinolines as small-molecule TLR7 agonists often suffer from their prompt dissemination and short half-life in the bloodstream, preventing their localization to the corresponding receptors and effective DC activation. We postulated that covalent incorporation of imidazoquinoline moieties onto the surface of biocompatible nanoparticles (~30 nm size) would enhance their chemical stability, cellular uptake efficiency, and adjuvanticity. The fully synthetic adjuvant-nanocomplexes led to successful DC activation at lower nanomolar doses compared with free small-molecule agonists. Once a model antigen such as ovalbumin was used for immunization, we found that the nanocomplexes promoted an unusually strong cytotoxic T lymphocyte response, revealing their unique immunostimulatory capacity benefiting from multivalency and efficient transport to endosomal TLR7.

■ INTRODUCTION

Dendritic cells (DCs) are the most potent antigen-presenting cells (APCs), which coordinate between the innate and adaptive immune systems.[1] They are specialized to engulf and process antigens and subsequently present epitopes to elicit robust immune responses.[2-4] APCs express various types of pattern recognition receptors including lectins or TLRs to distinguish between self- and non-self-structures. Recognition of pathogen associated molecular patterns (PAMPs) by TLRs generally induces DC activation.[5-7] Activated DCs present foreign epitopes of antigens onto major histocompatibility complexes (MHCs), and increase the expression of co-stimulatory molecules (CD80, CD86) to help cognate interaction with T cell receptor (TCR). The expression of chemokine receptor CCR7 leads DCs to migrate into lymph nodes, where naïve T cells are transformed into functional T lymphocytes

including cytotoxic T lymphocytes (CTLs).[8,9]

TLR7, located within endosomal compartment, is a promising adjuvant target-site for DC-mediated immunization. It recognizes nucleotide-derived compounds, including single-stranded RNA or low-molecular-weight imidazoquinoline derivatives, such as R837 (imiquimod) and R848 (resiquimod).[5,8,10] Yet, promotion of robust CTL responses by small-molecule adjuvants is highly challenging due to their prompt dissemination through diffusion.[8,11-13] To overcome these hurdles, polymeric or inorganic nanoparticles (NPs) encapsulating imidazoquinolines have been introduced to enhance stability and biodistribution of TLR7 agonists, consequently improving DC activation efficiency.[14-17] Here, we describe the first synthetic approach for preparing covalently linked imidazoquinoline-nanoconjugates for inducing robust CTL responses (**Figure 1**). Our design can entirely avoid the potential time-based release of small-molecule agonists from the non-covalently functionalized nanocarriers through the interactions between cell membranes and engineered NPs. However, the challenges associated with our approach are two-fold. First, the design of nanocomplexes requires multi-step reactions to achieve a molecularly well-defined structure. Second, the synthetic nanocomplexes should effectively initiate TLR-mediated DC activation and subsequently induce T cell immunity. To validate our working hypothesis, we designed alkyne-functionalized imidazoquinoline derivatives and covalently conjugated them with biocompatible NPs to examine their role in DC activation and generation of CTL response.

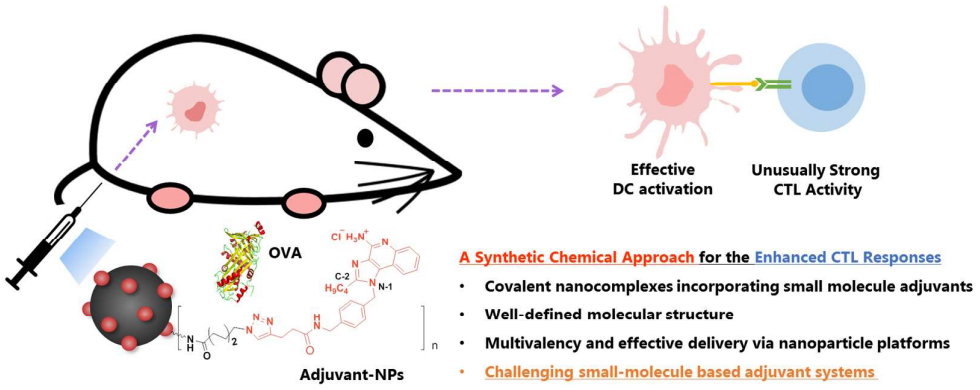

Figure 1. General attributes of Adjuvant-NPs in inducing DC activation and a robust CTL response.

■ RESULTS AND DISCUSSION

Although live-attenuated vaccines can elicit long-term immunity, they have a potential risk of infection, and practically not suitable vaccine candidates against pathogens such as influenza, HIV, or Ebola virus.[18] In contrast, subunit vaccines provide superior safety profiles and allow tunable design at the molecular-level to elicit predictable immune responses. However, they are short-lived and poorly immunogenic. Thus, immunostimulatory adjuvants are required to generate potent T cell immunity.[8,18] The advent of engineered nanocomplexes loaded with imidazoquinoline analogues opens up new opportunities to effectively target TLR7, yet investigations have been established on the basis of non-covalent encapsulation chemistry. Although CpG oligodeoxynucleotide-NP complexes have been previously demonstrated,[19,20] NPs covalently incorporating the small-molecule cognate ligands without repeating monomer units have not been reported so far.

To synthesize well-defined molecular adjuvant-nanocomplexes, we designed and prepared an imidazoquinoline analogue (Adjuvant **1**) with a terminal alkyne moiety to couple with azide coated iron oxide NPs (see **Figure 2**a). Adjuvant **2** was synthesized from 2,4-quinolinediol as previously described by the David group.[21-24] Based on the previous structure-activity relationship studies,[21,25-28] *n*-butyl group was introduced at C-2 position to increase TLR7 agonistic potency. Further, an alkyne functionality as a versatile anchor was placed at N-1 position for next-stage chemical reactions, since the site modification does not significantly compromise agonistic potency. Molecular structure of TLR7 agonist, Adjuvant **1**, was confirmed by ^{1}H and ^{13}C nuclear magnetic resonance (NMR) spectra (**Figures 2**b and **2**c). As a conjugation platform displaying multivalency, water-soluble and surface-engineered iron oxide NPs were selected because of their biocompatibility, facile surface modification, monodisperse size, biomolecule-free structure, and enhanced stability. In addition, they can be potentially applied as multifunctional agents for diagnostic/therapeutic purposes (e.g. magnetic resonance imaging (MRI) or photothermal therapy).[29-34] Biocompatible NPs with monodisperse size ranges of ~30 nm can be used as nanocarriers *in vivo*, which are optimal for internalization by immature DCs by facilitating endolysosomal pathway, and can be trafficked into the draining lymph nodes, thereby enhancing their adjuvanticity.[11,20,35-38] Amine-surface-modified iron oxide NPs (Amine-NPs) were then reacted with Spacer **3** with an activated ester moiety, to afford Azide-NPs, since azido functionality can be readily installed and is highly orthogonal and versatile for further transformations.

Finally, Adjuvant **1** was conjugated by Cu^{I}-catalyzed Huisgen 1,3-dipolar cycloaddition reaction, and treated with 0.1 M Tris buffer (pH 6) to form Adjuvant-NPs (for the details, see the Experimental Section and the Supporting Information).

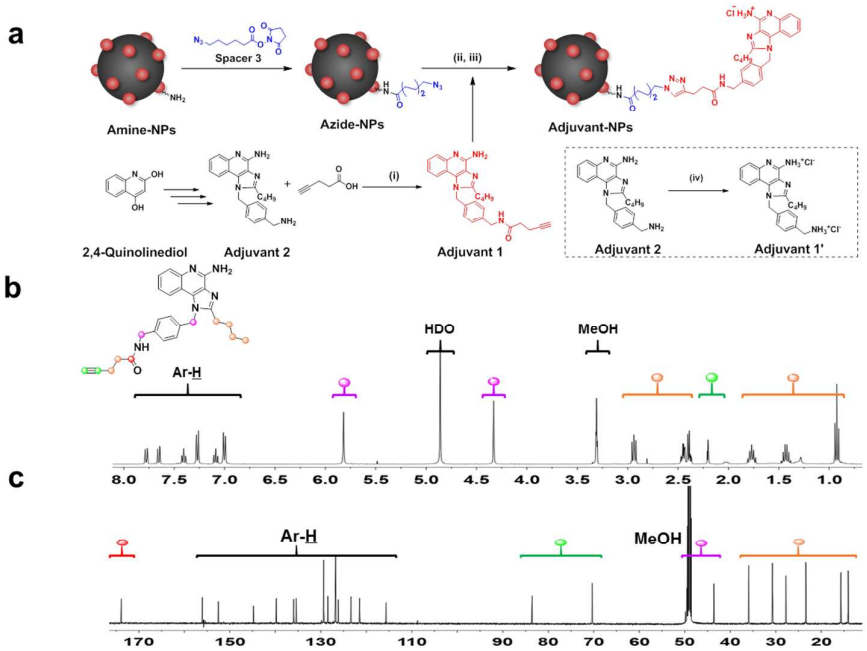

Figure 2. (a) Synthetic scheme of Adjuvant-NPs (i) HBTU, TEA, DCM, (ii) $CuSO_4 \cdot 5H_2O$, sodium ascorbate, DMF, (iii) 0.1 M Tris buffer (pH 6), (iv) diluted hydrogen chloride solution. (b, c) ^{1}H and ^{13}C NMR spectra (MeOD) of Adjuvant **1**.

Core- and hydrodynamic sizes of the synthetic nanocomplexes were determined by transmission electron microscopy (TEM) and dynamic light scattering (DLS) analyses, respectively (**Figures 3**a and **3**b). TEM image revealed spherical and monodisperse particles with ~11 nm core diameters of Adjuvant-NPs without any signs of particle aggregation, even after multi-step chemical modifications. DLS data analysis showed an effective diameter of 31.6 nm and a narrow size distribution with polydispersity index (PDI) = 0.258. Previously NPs having ~30 nm size have been demonstrated to be efficiently uptaken by DCs.[19,20] Moreover, we carried out spectroscopic studies to examine the effectiveness of imidazoquinoline conjugation. UV-Vis spectrum of Adjuvant-NPs showed distinct imidazoquinoline peaks at about 225, 246, and 321 nm with slight peak shifts (**Figure 3**c). To quantify the loading level, a fluorescence assay was conducted (**Figure 3**d), since iron oxide NPs are weakly fluorescent. NHS-fluorescein is an amine reactive fluorescent probe bearing an activated ester moiety, thus fluorophore can be appended to Adjuvant-NPs to generate Fluorescein-Adjuvant-NPs.

Based on the standard curve of NHS-fluorescein and iron concentration of NPs, the loading amount of imidazoquinolines in Adjuvant-NPs was estimated to be 0.139 μmol/[mg Fe] (see Supporting Information, Figures S1 and S2).

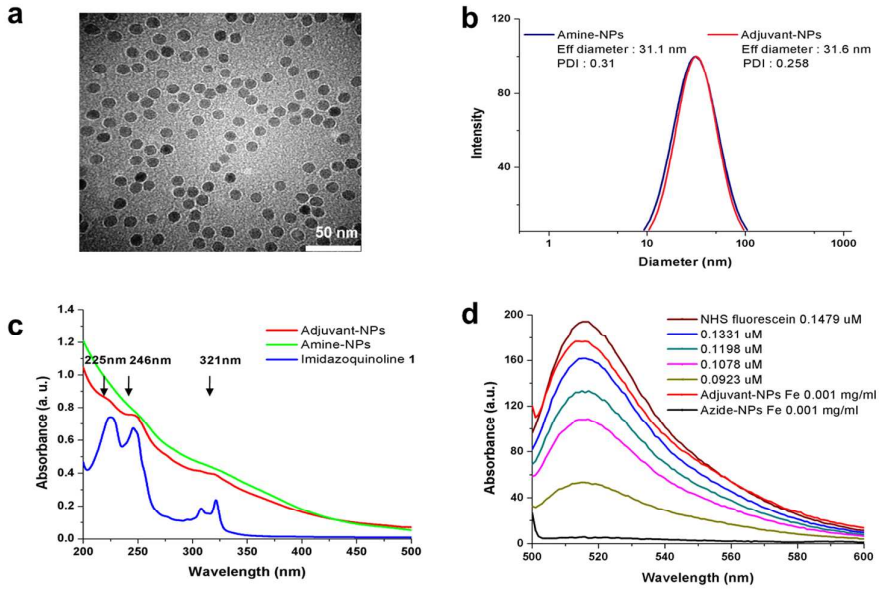

Figure 3. Characterization of Adjuvant-NPs. (a) TEM image of Adjuvant-NPs, (b) DLS analysis, (c) UV-Vis spectra, and (d) fluorescence spectra.

Further, we evaluated DC activation efficacies by using synthetic TLR7 agonists. Adjuvant-NPs or free Adjuvant **1'** were intraperitoneally injected into mice, and their DCs were harvested 18 hours later. DC activation markers including CD80, CD86, MHC I, and CCR7 were stained with phycoerythrin (PE)-conjugated antibodies and analyzed by flow cytometry. R848,[10] Adjuvant-NPs, or Adjuvant **1'** effectively increased the expression levels of the markers (**Figure 4** and Figures S3-S5). Highly water-soluble Adjuvant **1'** acted as an effective stimulant of DC activation at 115.6 nmol or even at a concentration as low as 69.4 nmol (Figure S3). Amine-NPs showed weak self-adjuvant effect (Figure S5). Remarkably, 13.9 nmol of Adjuvant-NPs (concentration in loading levels of cognate ligands) and 115.6 nmol of free Adjuvant **1'** induced comparable immunostimulatory activities. This is attributed to the enhanced avidity as well as effective internalization of the nanocomplexes to the endosomal TLR7 of DCs. IL-12p40 is known as one of important pro-inflammatory cytokines secreted from activated DCs to educate naïve $CD8^+$ T cells.[39] The secreted IL-12p40 levels of the Adjuvant-NP treated group were significantly higher than those of groups that were treated with PBS or Amine-NPs

(Figure S6a). Adjuvant **1'** also induced the production of the secreted IL-12p40 with an almost identical level. To directly detect the antigen-specific $CD8^+$ T cell response, we carried out MHC I tetramer assays and observed increased populations of OT-1 peptide-specific $CD8^+$ T cells in the groups treated with Adjuvant **1'** or Adjuvant-NPs compared to those of Amine-NPs (Figure S6b). These data suggested that adjuvant-NPs induce efficient DC activation leading to the effective presentation of antigenic peptides on MHC I and subsequent antigen-specific CTL effect.

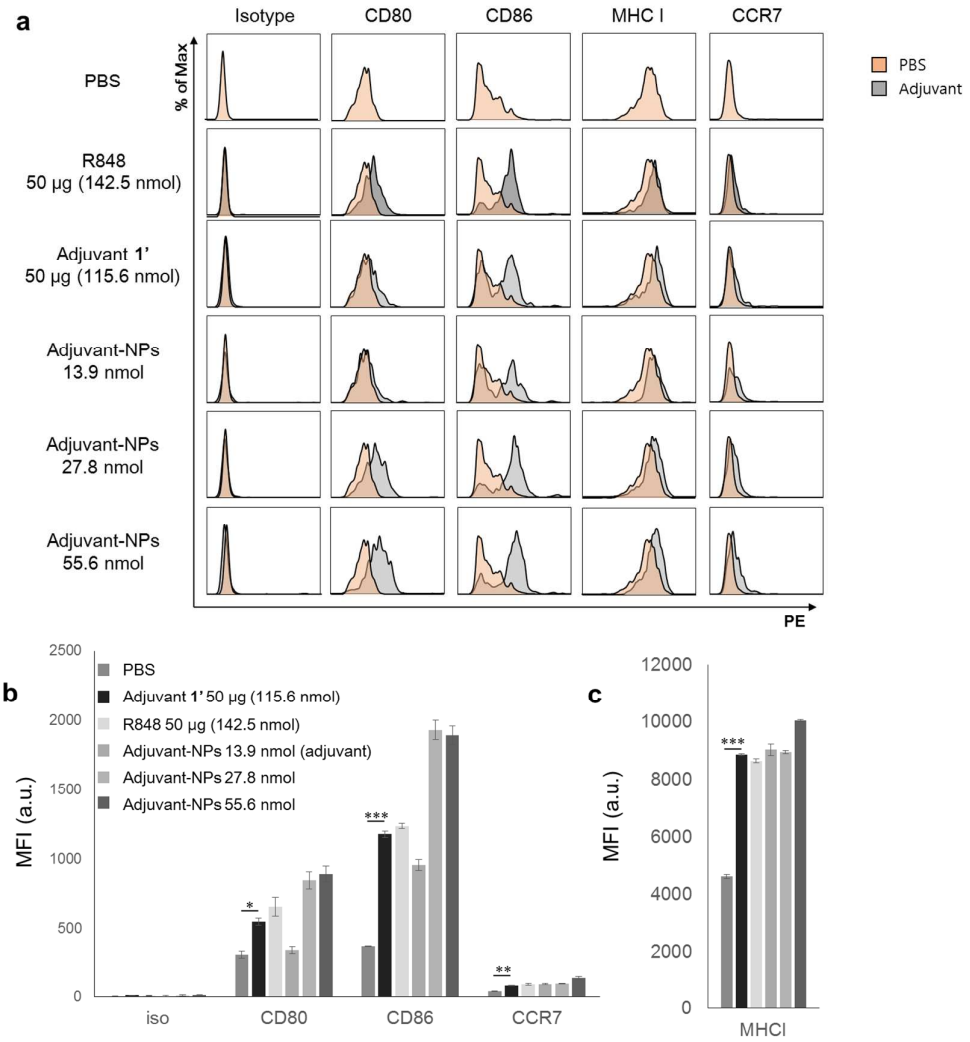

Figure 4. Adjuvant effects on *in vivo* DC activation. (a) flow cytometry analyses, and (b and c) the mean fluorescence intensity (MFI) levels of DC activation markers (CD80, CD86, CCR7, and MHC I). The P values < 0.05(*) <0.01(**) <0.001(***) were considered significant.

Since TLR7 is expressed inside endosomal compartments of DCs, effective delivery of antigens and adjuvants into DCs is indispensable for their proper maturation and subsequent immune

response. However, free small molecules hardly localize to TLRs; thus, they require effective delivery vehicles. To examine cellular internalization of the nanocomplexes and their appropriate localization in DCs, we prepared Fluorescein-Adjuvant-NPs as probes (see Supporting Information) and studied their uptake using confocal fluorescence microscopy (**Figure 5**a). The complexes were cultured with immature DCs *in vitro* in the presence of ovalbumin (OVA) as a model antigen. After 18 hours, the cells were fixed, and the nuclei and low pH endosomes were stained with DAPI and LysoTracker, respectively. Fluorescent confocal cell images clearly demonstrated that Fluorescein-Adjuvant-NPs were localized within endosomes thanks to their suitable particle size (~30 nm) (**Figure 5**b and Figure S7),[19,20] which can assist imidazoquinoline cognate agonists effectively interact with TLR7 within DC endosomes.

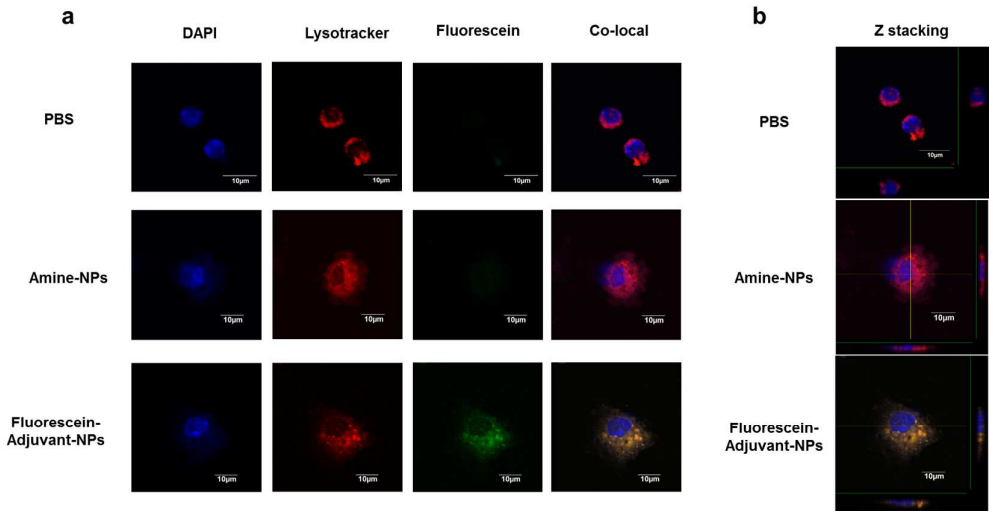

Figure 5. (a and b) Fluorescence imaging studies to examine the internalization of Fluorescein-Adjuvant-NPs in DCs. Samples were characterized by confocal fluorescent microscopy.

The efficient DC activation and nanocomplex internalization prompted us to test whether these mature DCs can elicit sufficient cytotoxic $CD8^+$ T cell responses. We performed an *in vivo* CTL assay based on the carboxyfluorescein diacetate succinimidyl ester (CFSE) assay to monitor OVA-specific T cell proliferation.[40,41] Mice were intraperitoneally immunized with 25 μg of OVA protein as an antigen in the presence of PBS, R848, Amine-NPs, or Adjuvant-NPs as TLR7 agonists. Groups of mice were primarily immunized for 2 weeks, and additionally boosted for 1 week. After immunization, mice were intravenously injected with 50:50 mixtures of OT-1 peptide-pulsed ($CFSE^{hi}$) and unpulsed ($CFSE^{low}$) syngeneic splenocytes to evaluate OVA-specific CTL activity. The population of OT-1

peptide pulsed target cells was analyzed by flow cytometry. It is speculated that if OT-1 specific T cells are effectively stimulated by matured DCs with OVA protein and adjuvants, the percentage of OT-1 peptide-pulsed ($CFSE^{hi}$) syngeneic splenocytes would be lysed and their population decreased because of T cell cytotoxicity (**Figure 6**a). Remarkably, injection of Adjuvant-NPs with 27.8 nmol of adjuvant together with OVA protein caused 84% target cell lysis. In contrast, small-molecule R848 (28.5 or 142.5 nmol) or Amine-NPs showed negligible to poor (0-25%) cytotoxic responses (**Figure 6**b). It is speculated that superior $CD8^+$ T cell efficacy of Adjuvant-NPs at low doses of imidazoquinoline moiety is associated with the enhanced avidity of fully synthesized multivalent adjuvant-NPs and effective DC internalization.

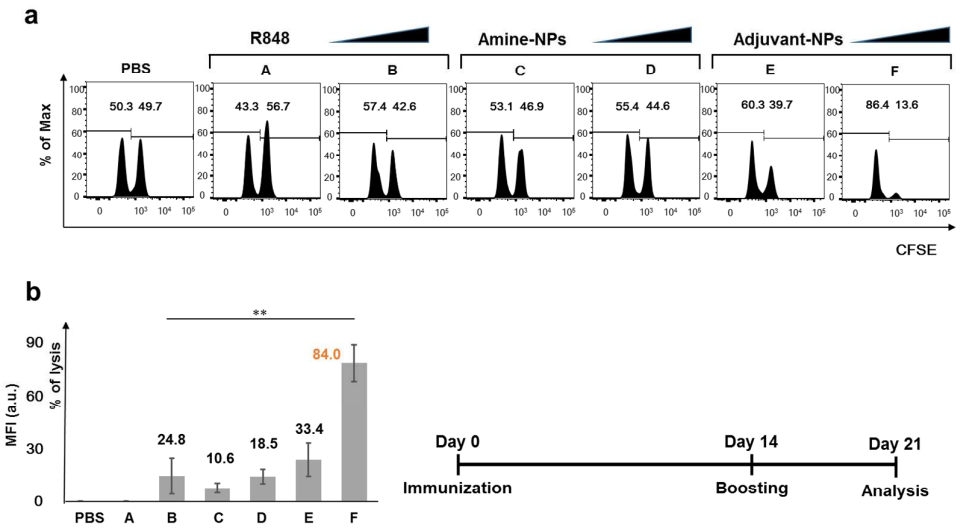

Figure 6. *In vivo* CTL assay on splenocytes. (a) Percentages of OT-1 peptide unpulsed $CFSE^{low}$ (left) and that of pulsed $CFSE^{high}$ (right) were analyzed by flow cytometry. Each group was stimulated with indicated adjuvants; Sample A: R848 10 μg, 28.5 nmol; sample B: R 848 50 μg, 142.5 nmol; sample C: amine-NPs 100 μg Fe; sample D: amine NPs 200 μg Fe; sample E: Adjuvant-NPs (100 μg Fe, 13.9 nmol of imidazoquinoline); sample F: Adjuvant-NPs (200 μg Fe, 27.8 nmol of imidazoquinoline) along with OVA protein. (b) The conversion of the percentages of $CFSE^{high}$ based on the negative control of PBS treated group. The P values < 0.01(**) were considered significant.

■ CONCLUSION

We chemically synthesized structurally well-defined molecular adjuvant-nanoparticle conjugates through multi-step reactions and investigated their potency of their immunostimulatory activity. The nanocomplexes displaying multiple low-molecular-weight ligands were efficiently internalized by

immature DCs, and they subsequently enhanced *in vivo* DC activation by facilitating multivalent interactions between imidazoquinoline moieties and endosomal TLR7. In addition, they induced increased expression levels of activation markers in the low nanomolar range. Their cellular localization was validated by fluorescent labeling of the nanocomplexes. Co-administration of the synthetic adjuvant-nanocomplexes and OVA protein elicited unusually robust antigen-specific cytotoxic T cell responses. Considering the significant challenges generating cell-mediated immunity via small-molecule based adjuvant systems, we believe that our synthetic approach can provide a versatile platform for the rational designing of next-generation vaccines.

■ EXPERIMENTAL SECTION

Synthesis of Adjuvant **1**: Adjuvant **2**[21] (400 mg, 1.11 mmol) and TEA (547 μL, 3.89 mmol, 3.5 equiv) were dissolved in DCM (80 mL). 4-pentynoic acid (142 mg, 1.45 mmol, 1.3 equiv) and HBTU (549 mg, 1.45 mmol, 1.3 equiv) were added at 0 °C, and the solution left to stir overnight at room temperature. The reaction mixture was concentrated *in vacuo* and the residue was purified by flash column chromatography (DCM:MeOH:NH_4OH = 9.5:0.5:0.1) to yield the title compound as a clear oil (261 mg, 53%). ^{1}H NMR (400 MHz, MeOD) δ_H 0.92 (t, *J* 7.4 Hz, 3H), 1.42 (dt, *J* 14.7, 7.4 Hz, 2H), 1.77 (dt, *J* 15.4, 7.6 Hz, 2H), 2.20 (t, *J* 2.6 Hz, 1H), 2.34-2.49 (m, 4H), 4.33 (s, 2H), 5.82 (s, 2H), 7.00 (d, *J* 8.1 Hz, 2H), 7.09 (m, 1H), 7.27 (d, *J* 8.1 Hz, 2H), 7.41 (m, 1H), 7.65 (dd, *J* 8.3, 0.4 Hz, 1H), 7.78 (d, *J* 7.8 Hz, 1H); ^{13}C NMR (150 MHz, MeOD) δ_C 14.1, 15.7, 23.4, 27.8, 30.7, 35.9, 43.6, 49.5, 70.3, 83.5, 115.7, 121.5, 123.4, 126.2, 126.7, 126.9 128.5 129.4 135.4, 136.0, 139.8, 144.8, 152.5, 156.0, 173.8.; HRMS (ESI): Calcd for $C_{27}H_{30}N_5O^+$ $[M+H]^+$: 440.2445, found 440.2445.

Synthesis of Azido-NPs: Spacer **3**[42] (30 mg, 116 μmol) dissolved in DMF was added to the Amine-NPs (1.5 mg Fe). Mixture was stirred at room temperature for a day, then dialyzed in DI water was conducted for 3 times to remove non-conjugated molecules in excess.

Synthesis of Adjuvant-NPs: Adjuvant **1** (2.55 mg, 5.80 μmol, 15 equiv) dissolved in DMF, $CuSO_4{\cdot}6H_2O$ (1.45 mg, 5.80 μmol, 15 equiv) and (+)-sodium L-ascorbate (1.15 mg, 5.80 μmol, 15 equiv) was added to Azide-NPs and stirred at room temperature for a day. The reaction mixture was

dialyzed in DI water for two times then, treated with 0.1 M Tris buffer (pH 6) for 2 times to form ammonium salt of imidazoquinoline moiety. Solution was filtered through 0.2 μm pore size filter and concentrated to 3 mg/mL Fe dissolved in autoclaved PBS buffer by using centrifugal filter (3000 rpm, 12 min).

■ ASSOCIATED CONTENT

Supporting Information

The Supporting Information is available free of charge on the ACS Publications website at DOI: 10.1021/acs.bioconjchem.xxxxxxx. Details of synthetic and immunological experimental procedures and NMR spectra are provided (PDF)

■ AUTHOR INFORMATION

Corresponding Authors

*Email: sabsab7@unist.ac.kr

*Email: syhong@unist.ac.kr

Authors Contributions

[§]W.G.K. and B.C. contributed equally to this work. W.G.K., B.C., S.K. and S.Y.H. designed the research project. W.G.K., B.C., H.-J.Y., J.-A.H., H.J. performed the experiments, W.G.K., B.C., H.-J.Y., J.-A.H., H.J., H.C., S.K., and S.Y.H. analyzed the data, and W.G.K., B.C., S.K., and S.Y.H. wrote the paper.

Notes

The authors declare no competing financial interests.

■ ACKNOWLEDGMENTS

This work was supported by National Research Foundation of Korea (NRF-2016K1A3A1A25003511 and NRF-2010-0028684). Authors are grateful to Prof. Francesco Peri for many helpful discussions.

■ REFERENCES

(1) Tacken, P. J., de Vries, I. J. M., Torensma, R. and Figdor, C. G. (2007) Dendritic-cell immunotherapy: from ex vivo loading to *in vivo* targeting. *Nat. Rev. Immunol. 7*, 790-802.
(2) Palucka, K. and Banchereau, J. (2012) Cancer immunotherapy via dendritic cells. *Nat. Rev. Cancer 12*, 265-277.
(3) Mandal, S., Hammink, R., Tel, J., Eksteen-Akeroyd, Z. H., Rowan, A. E., Blank, K. and Figdor, C. G. (2015) Polymer-based synthetic dendritic cells for tailoring robust and multifunctional T cell responses. *ACS Chem. Biol. 10*, 485-492.
(4) Mandal, S., Eksteen-Akeroyd, Z. H., Jacobs, M. J., Hammink, R., Koepf, M., Lambeck, A. J. A., van Hest, J. C. M., Wilson, C. J., Blank, K., Figdor, C. G. *et al*. (2013) Therapeutic nanoworms: towards novel synthetic dendritic cells for immunotherapy. *Chem. Sci. 4*, 4168-4174.
(5) O'Neill, L. A. J., Golenbock, D. and Bowie, A. G. (2013) The history of Toll-like receptors-redefining innate immunity. *Nat. Rev. Immunol. 13*, 453-460.
(6) Iwasaki, A. and Medzhitov, R. (2010) Regulation of adaptive immunity by the innate immune system. *Science 327*, 291-295.
(7) Tom, J. K., Dotsey, E. Y., Wong, H. Y., Stutts, L., Moore, T., Davies, D. H., Felgner, P. L. and Esser-Kahn, A. P. (2015) Modulation of innate immune responses *via* covalently linked TLR agonists. *ACS Cent. Sci. 1*, 439-448.
(8) Moyle, P. M. and Toth, I. (2013) Modern subunit vaccines: development, components, and research opportunities. *ChemMedChem 8*, 360-376.
(9) Palucka, K., Banchereau, J. and Mellman, I. (2010) Designing vaccines based on biology of human dendritic cell subsets. *Immunity 33*, 464-478.
(10) Hemmi, H., Kaisho, T., Takeuchi, O., Sato, S., Sanjo, H., Hoshino, K., Horiuchi, T., Tomizawa, H., Takeda, K. and Akira, S. (2002) Small anti-viral compounds activate immune cells via the TLR7 MyD88-dependent signaling pathway. *Nat. Immunol. 3*, 196-200.
(11) Moon, J. J., Huang, B. and Irvine, D. J. (2012) Engineering nano- and microparticles to tune immunity. *Adv. Mater. 24*, 3724-3746.
(12) Rajagopal, D., Paturel, C., Morel, Y., Uematsu, S., Akira, S. and Diebold, S. S. (2010) Plasmacytoid dendritic cell-derived type I interferon is crucial for the adjuvant activity of Toll-like receptor 7 agonists. *Blood 115*, 1949-1957.
(13) Warshakoon, H. J., Hood, J. D., Kimbrell, M. R., Malladi, S., Wu, W. Y., Shukla, N. M., Agnihotri, G., Sil, D. and David, S. A. (2009) Potential adjuvantic properties of innate immune stimuli. *Hum. Vaccin. 5*, 381-394.
(14) Kasturi, S. P., Skountzou, I., Albrecht, R. A., Koutsonanos, D., Hua, T., Kakaya, H. I., Ravindran, R., Stewart, S., Alam, M., Kwissa, M. *et al*. (2011) Programming the magnitude and persistence of antibody responses with innate immunity. *Nature 470*, 543-550.
(15) Heo, M. B. and Lim, Y. T. (2014) Programmed nanoparticles for combined immunomodulation, antigen presentation and tracking of immunotherapeutic cells. *Biomaterials 35*, 590-600.
(16) Ilyinskii, P. O., Roy, C. J., O'Neil, C. P., Browning, E. A., Pittet, L. A., Altreuter, D. H., Alexis, F., Tonti, E., Shi, J., Basto, P. A. *et al*. (2014) Adjuvant-carrying synthetic vaccine particles augment the immune response to encapsulated antigen and exhibit strong local immune activation without inducing systemic cytokine release. *Vaccine 32*, 2882-2895.
(17) Tacken, P. J., Zeelenberg, I. S., Cruz, L. J., van Hout-Kuijer, M. A., van de Glind, G., Fokkink, R. G., Lambeck, A. J. A. and Figdor, C. G. (2011) Targeted delivery of TLR ligands to human and mouse dendritic cells strongly enhances adjuvanticity. *Blood 118*, 6836-6844.
(18) Coffman, R. L., Sher, A. and Seder, R. A. (2010) Vaccine adjuvants: putting innate immunity to work. *Immunity 33*, 492-503.
(19) de Titta, A., Ballester, M., Julier, Z., Nembrini, C., Jeanbart, L., van der Vlies, A. J., Swartz, M. A. and Hubbell, J. A. (2013) Nanoparticle conjugation of CpG enhances adjuvancy for cellular immunity and memory recall at low dose. *Proc. Natl. Acad. Sci. U.S.A. 110*, 19902-19907.
(20) Molino, N. M., Anderson, A. K. L., Nelson, E. L. and Wang, S.-W. (2013) Biomimetic protein nanoparticles facilitate enhanced dendritic cell activation and cross-presentation. *ACS Nano 7*, 9743-9752.
(21) Shukla, N. M., Malladi, S. S., Mutz, C. A., Balakrishna, R. and David, S. A. (2010) Structure-activity relationships in human toll-like receptor 7-active imidazoquinoline analogues. *J. Med. Chem. 53*, 4450-4465.
(22) Shukla, N. M., Mutz, C. A., Ukani, R., Warshakoon, H. J., Moore, D. S. and David, S. A. (2010) Syntheses of fluorescent imidazoquinoline conjugates as probes of Toll-like receptor 7. *Bioorg. Med. Chem. Lett. 20*, 6384-6386.
(23) Shukla, N. M., Lewis, T. C., Day, T. P., Mutz, C. A., Ukani, R., Hamilton, C. D., Balakrishna, R. and David, S. A. (2011) Toward self-adjuvanting subunit vaccines: model peptide and protein antigens incorporating covalently bound toll-like receptor-7 agonistic imidazoquinolines. *Bioorg. Med. Chem. Lett. 21*, 3232-3236.
(24) Shukla, N. M., Mutz, C. A., Malladi, S. S., Warshakoon, H. J., Balakrishna, R. and David, S. A. (2012) Toll-like receptor (TLR)-7 and -8 modulatory activities of dimeric imidazoquinolines. *J. Med. Chem. 55*, 1106-1116.
(25) Schiaffo, C. E., Shi, C., Xiong, Z., Olin, M., Ohlfest, J. R., Aldrich, C. C. and Ferguson, D. M. (2014) Structure-activity relationship analysis of imidazoquinolines with Toll-like receptors 7 and 8 selectivity and enhanced cytokine induction. *J. Med. Chem. 57*, 339-347.
(26) Shi, C., Xiong, Z., Chittepu, P., Aldrich, C. C., Ohlfest, J. R. and Ferguson, D. M. (2012) Discovery of imidazoquinolines with Toll-like receptor 7/8 independent cytokine induction. *ACS Med. Chem. Lett. 3*, 501-504.
(27) Ryu, K. A., Stutts, L., Tom, J. K., Mancini, R. J. and Esser-Kahn, A. P. J. (2014) Stimulation of innate immune cells by light-activated TLR7/8 agonists. *J. Am. Chem. Soc. 136*, 10823-10825.

(28) Yoo, E., Salunke, D. B., Sil, D., Guo, X., Salyer, A. C. D., Hermanson, A. R., Kumar, M., Malladi, S. S., Balakrishna, R., Thompson, W. H. *et al*. (2014) Determinants of activity at human Toll-like receptors 7 and 8: quantitative structure-activity relationship (QSAR) of diverse heterocyclic scaffolds. *J. Med. Chem. 57*, 7955-7970.
(29) Dobrovolskaia, M. A. and McNeil, S. E. (2007) Immunological properties of engineered nanomaterials. *Nat. Nanotech. 2*, 469-478.
(30) Gupta, A. K. and Gupta, M. (2005) Synthesis and surface engineering of iron oxide nanoparticles for biomedical applications. *Biomaterials 26*, 3995-4021.
(31) Na, H. B., Song, I. C. and Hyeon, T. (2009) Inorganic nanoparticles for MRI contrast agents. *Adv. Mater. 21*, 2133-2148.
(32) de Vries, I. J. M., Lesterhuis, W. J., Barentsz, J. O., Verdijk, P., van Krieken, J. H., Boerman, O. C., Oyen, W. J., Bonenkamp, J. J., Boezeman, J. B., Adema, G. J. *et al*. (2005) Magnetic resonance tracking of dendritic cells in melanoma patients for monitoring of cellular therapy. *Nat. Biotechnol. 23*, 1407-1413.
(33) Song, X., Gong, H., Yin, S., Cheng, L., Wang, C., Li, Z., Li, Y., Wang, X., Liu, G. and Liu, Z. (2014) Ultra-small iron oxide doped polypyrrole nanoparticles for *in vivo* multimodal imaging guided photothermal therapy. *Adv. Funct. Mater. 24*, 1194-1201.
(34) Yang, K., Hu, L., Ma, X., Ye, S., Cheng, L., Shi, X., Li, C., Li, Y. and Liu, Z. (2012) Multimodal imaging guided photothermal therapy using functionalized graphene nanosheets anchored with magnetic nanoparticles. *Adv. Mater. 24*, 1868-1872.
(35) Irvine, D. J., Hanson, M. C., Rakhra, K. and Tokatlian, T. (2015) Synthetic nanoparticles for vaccines and immunotherapy. *Chem. Rev. 115*, 11109-11146.
(36) Leleux, J. and Roy, K. (2013) Micro and nanoparticle-based delivery systems for vaccine immunotherapy: an immunological and materials perspective. *Adv. Healthcare Mater. 2*, 72-94.
(37) Mintern, J. D., Percival, C., Kamphuis, M. M. J., Chin, W. J., Caruso, F. and Johnston, A. P. R. (2013) Targeting dendritic cells: the role of specific receptors in the internalization of polymer capsules. *Adv. Healthcare Mater. 2*, 940-944.
(38) Smith, D. M., Simon, J. K. and Baker, J. R. (2013) Applications of nanotechnology for immunology. *Nat. Rev. Immunol. 13*, 592-605.
(39) Koch, F., Stanzl, U., Jennewein, P., Janke, K., Heufler, C., Kampgen, E., Romani, N. and Schuler, G. (1996) High level IL-12 production by murine dendritic cells: upregulation via MHC class II and CD40 molecules and downregulation by IL-4 and IL-10. *J. Exp. Med. 184*, 741-746.
(40) Han, J.-A., Kang, Y. J., Shin, C., Ra, J.-S., Shin, H.-H., Hong, S. Y., Do, Y. and Kang, S. (2014) Ferritin protein cage nanoparticles as versatile antigen delivery nanoplatforms for dendritic cell (DC)-based vaccine development. *Nanomedicine 10*, 561-569.
(41) Quah, B. J. C., Warren, H. S. and Parish, C. R. (2007) Monitoring lymphocyte proliferation in vitro and *in vivo* with the intracellular fluorescent dye carboxyfluorescein diacetate succinimidyl ester. *Nat. Protoc. 2*, 2049-2056.
(42) Lampkins, A. J., O'Neil, E. J. and Smith, B. D. (2008) Bio-orthogonal phosphatidylserine conjugates for delivery and imaging applications. *J. Org. Chem. 73*, 6053-6058.

TOC Image

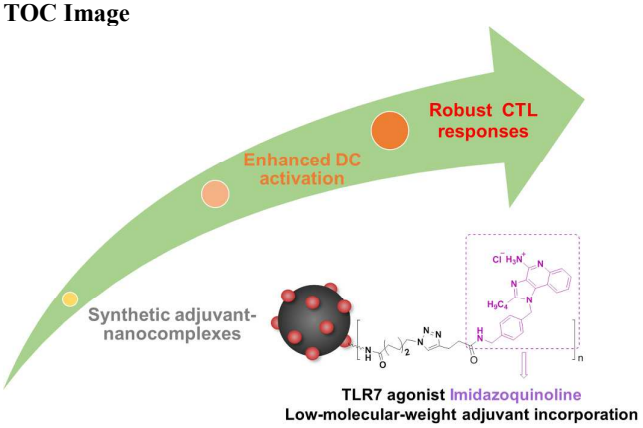

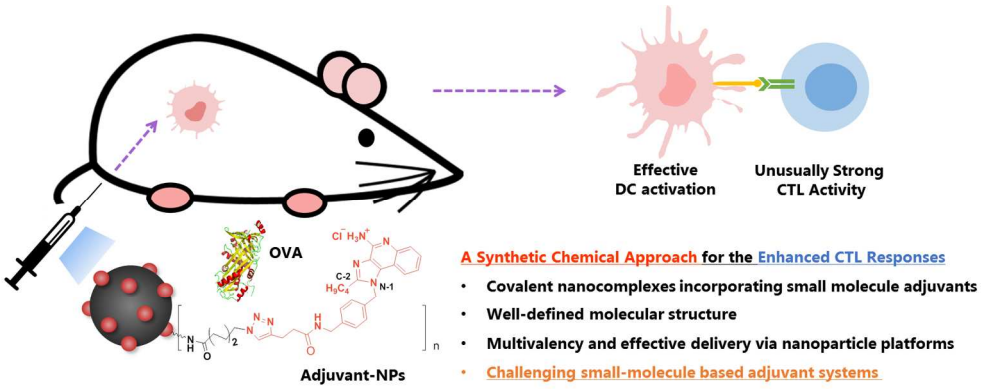

Figure 1. General attributes of Adjuvant-NPs in inducing DC activation and a robust CTL response.

308x120mm (150 x 150 DPI)

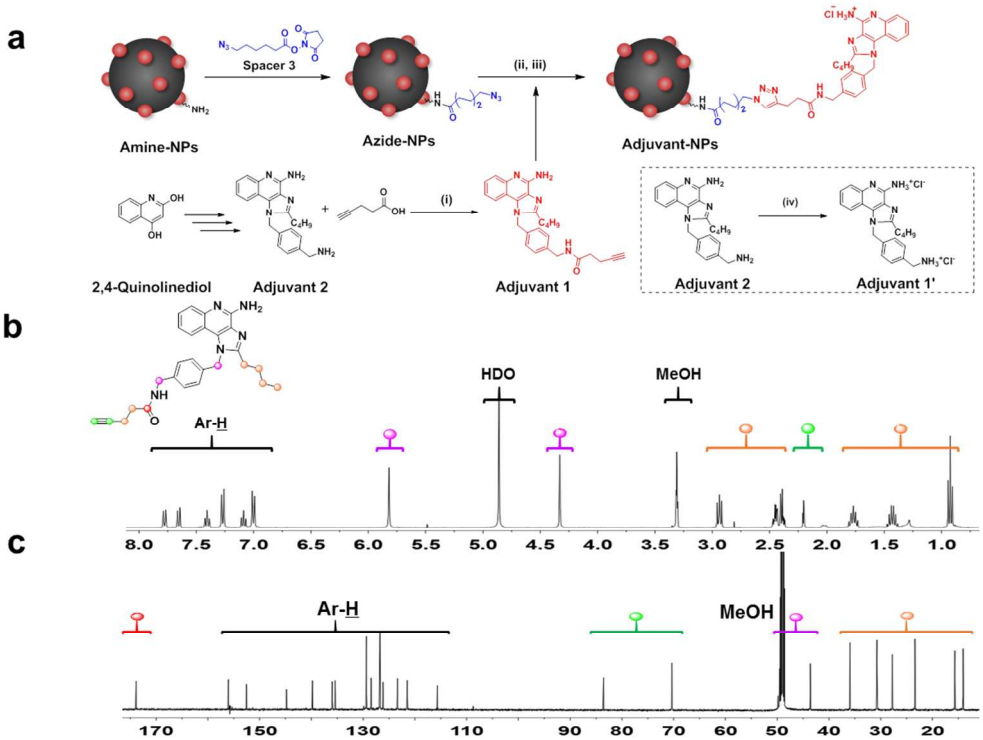

Figure 2. (a) Synthetic scheme of Adjuvant-NPs (i) HBTU, TEA, DCM, (ii) CuSO4 5H2O, sodium ascorbate, DMF, (iii) 0.1 M Tris buffer (pH 6), (iv) diluted hydrogen chloride solution. (b, c) 1H and 13C NMR spectra (MeOD) of Adjuvant 1.

207x152mm (150 x 150 DPI)

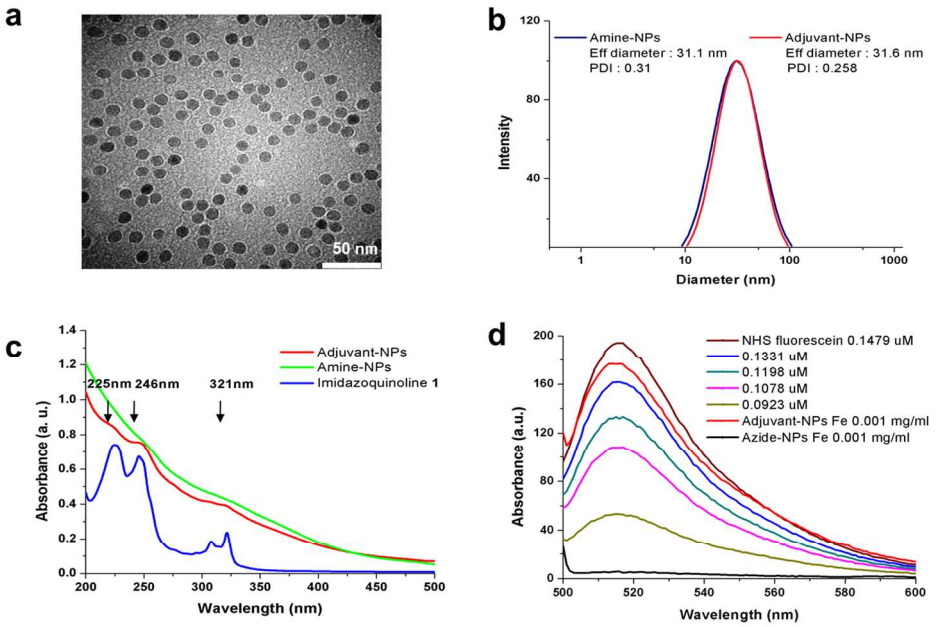

Figure 3. Characterization of Adjuvant-NPs. (a) TEM image of Adjuvant-NPs, (b) DLS analysis, (c) UV-Vis spectra, and (d) fluorescence spectra.

246x160mm (150 x 150 DPI)

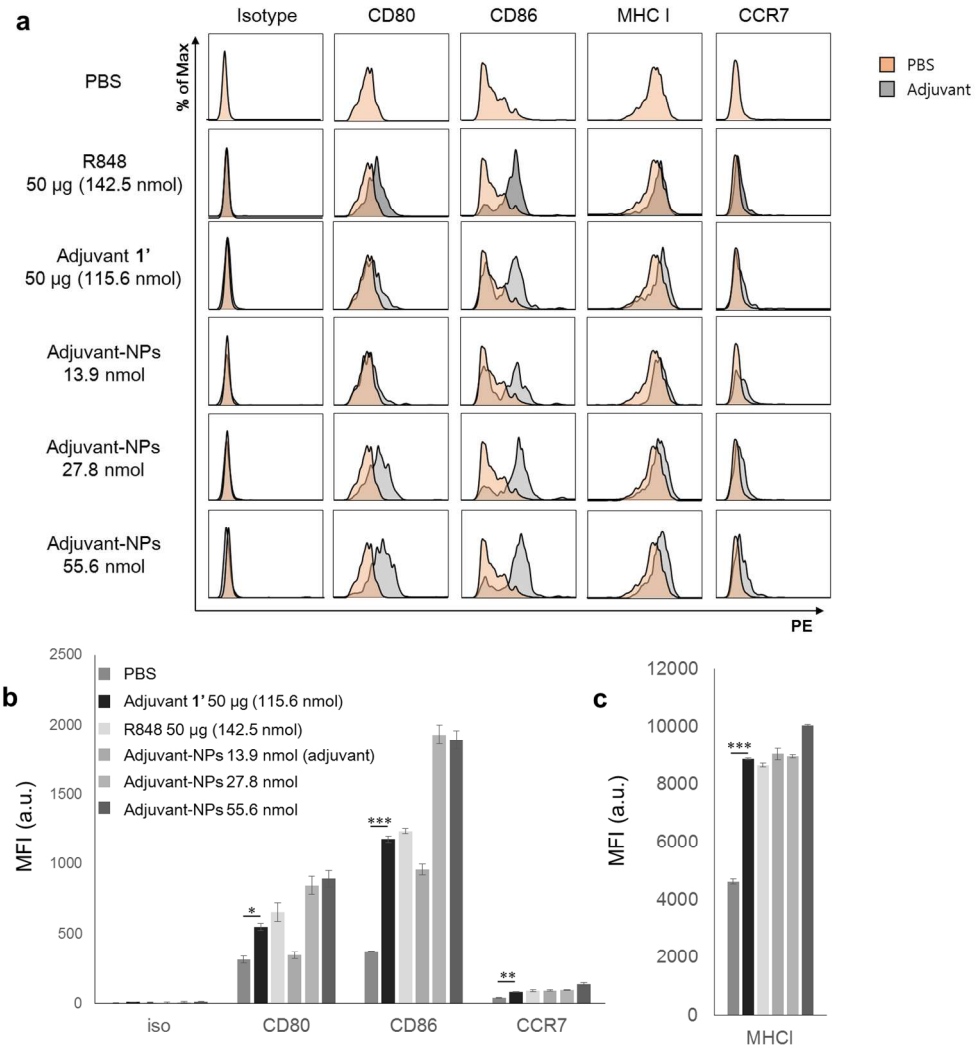

Figure 4. Adjuvant effects on in vivo DC activation. (a) flow cytometry analyses, and (b and c) the mean fluorescence intensity (MFI) levels of DC activation markers (CD80, CD86, CCR7, and MHC I). The P values < 0.05(*) <0.01(**) <0.001(***) were considered significant.

262x278mm (150 x 150 DPI)

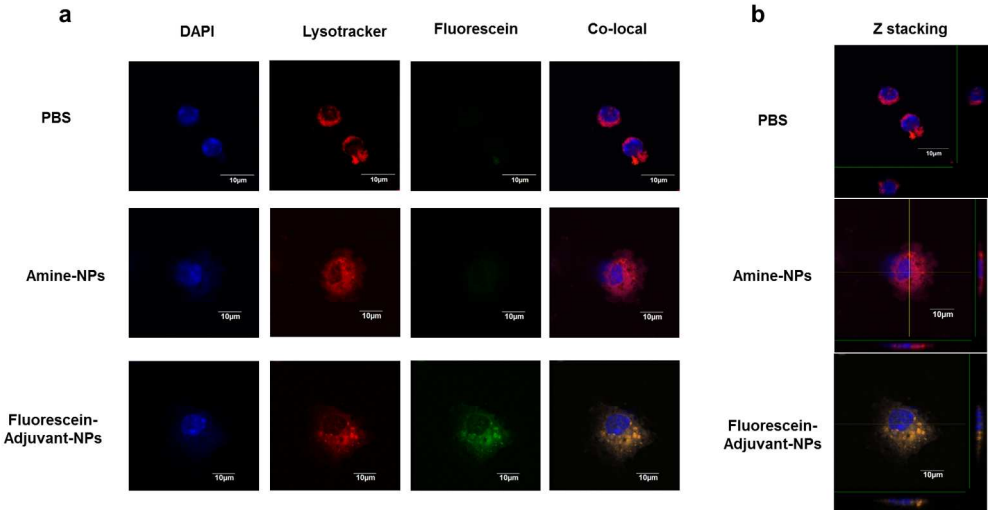

Figure 5. (a and b) Fluorescence imaging studies to examine the internalization of Fluorescein-Adjuvant-NPs in DCs. Samples were characterized by confocal fluorescent microscopy.

327x169mm (150 x 150 DPI)

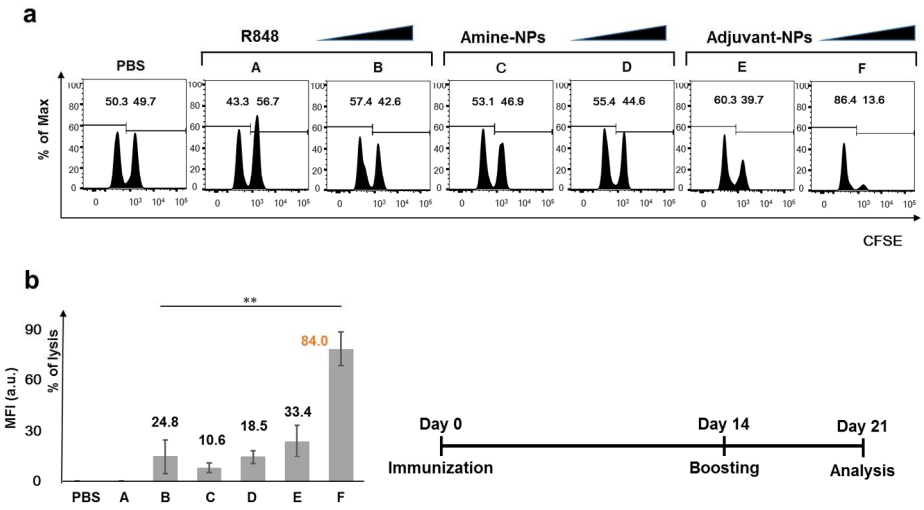

Figure 6. In vivo CTL assay on splenocytes. (a) Percentages of OT-1 peptide unpulsed CFSElow (left) and that of pulsed CFSEhigh (right) were analyzed by flow cytometry. Each group was stimulated with indicated adjuvants; Sample A: R848 10 μg, 28.5 nmol; sample B: R 848 50 μg, 142.5 nmol; sample C: amine-NPs 100 μg Fe; sample D: amine NPs 200 μg Fe; sample E: Adjuvant-NPs (100 μg Fe, 13.9 nmol of imidazoquinoline); sample F: Adjuvant-NPs (200 μg Fe, 27.8 nmol of imidazoquinoline) along with OVA protein. (b) The conversion of the percentages of CFSEhigh based on the negative control of PBS treated group. The P values < 0.01(**) were considered significant.

303x169mm (150 x 150 DPI)

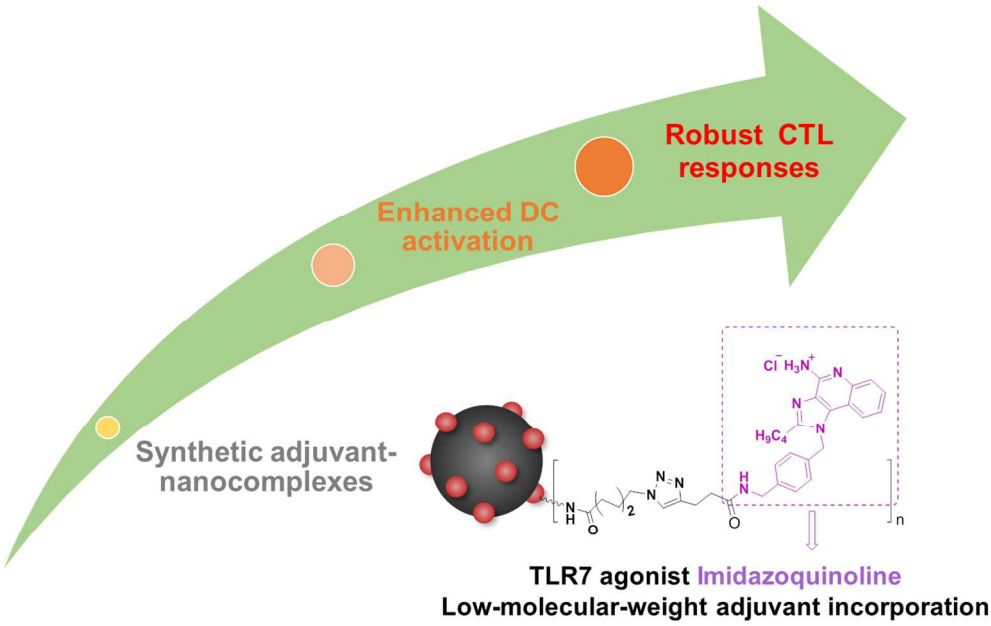

TOC image

250x157mm (150 x 150 DPI)